Spectroscopic and Kinetic Properties of Recombinant Choline Oxidase from *Arthrobacter globiformis*†

Mahmoud Ghanem,[‡,§] Fan Fan,[§,||] Kevin Francis,[||] and Giovanni Gadda*[,‡,||,⊥]

Departments of Chemistry and Biology, and The Center for Biotechnology and Drug Design, Georgia State University, Atlanta, Georgia 30302-4098

Received August 12, 2003; Revised Manuscript Received October 25, 2003

ABSTRACT: Choline oxidase catalyzes the four-electron oxidation of choline to glycine betaine, with molecular oxygen acting as primary electron acceptor. Recently, the recombinant enzyme expressed in *Escherichia coli* was purified to homogeneity and shown to contain FAD in a mixture of oxidized and anionic semiquinone redox states [Fan et al. (2003) *Arch. Biochem. Biophys.*, in press]. In this study, methods have been devised to convert the enzyme-bound flavin semiquinone to oxidized FAD and vice versa, allowing characterization of the resulting forms of choline oxidase. The enzyme-bound oxidized flavin showed typical UV−vis absorbance peaks at 359 and 452 nm (with $\epsilon_{452} = 11.4\ M^{-1}\ cm^{-1}$) and emitted light at 530 nm (with λ_{ex} at 452 nm). The affinity of the enzyme for sulfite was high (with a K_d value of ∼50 μM at pH 7 and 15 °C), suggesting the presence of a positive charge near the N(1)C(2)═O locus of the flavin. The enzyme-bound anionic flavin semiquinone was unusually insensitive to oxygen or ferricyanide at pH 8 and showed absorbance peaks at 372 and 495 nm (with $\epsilon_{372} = 19.95\ M^{-1}\ cm^{-1}$), maximal fluorescence emission at 454 nm (with λ_{ex} at 372 nm), circular dichroic signals at 370 and 406 nm, and an ESR peak-to-peak line width of 13.9 G. Both UV−vis absorbance studies on the enzyme under turnover with choline and steady-state kinetic data with either choline or betaine aldehyde were consistent with the flavin semiquinone being not involved in catalysis. The pH dependence of the kinetic parameters at varying concentrations of both choline and oxygen indicated that a catalytic base is required for choline oxidation but not for oxygen reduction and that the order of the kinetic steps involving substrate binding and product release is not affected by pH.

Choline oxidase (EC 1.1.3.17) catalyzes the four-electron oxidation of choline to glycine betaine (*N*,*N*,*N*-trimethylglycine; betaine) via betaine aldehyde as intermediate (Scheme 1) (*1*). The enzyme contains covalently bound FAD and utilizes molecular oxygen as the primary electron acceptor (*2*−*4*). Among the members of the GMC oxidoreductase superfamily within which the enzyme can be grouped (*5*, *6*), choline oxidase is unique in that it catalyzes the oxidation of a substrate primary alcohol to a carboxylic acid via an aldehyde intermediate. A similar oxidation reaction of an alcohol to a carboxylic acid is catalyzed by histidinol dehydrogenase (EC 1.1.1.23), a pyridine nucleotide-dependent enzyme well-characterized in its mechanistic and biochemical properties (*7*−*17*). In contrast, limited kinetic information is available on choline oxidase (*18*, *19*). Consequently, the study of the mechanistic properties of choline oxidase provides the opportunity to compare the biochemical and mechanistic properties of the flavin-dependent oxidoreductases with those of the pyridine nucleotide-dependent reductases able to carry out a four-electron oxidation of a substrate alcohol. The study of an enzyme involved in glycine betaine biosynthesis is also of considerable interest for both biotechnological and biomedical applications because recent studies have shown that the accumulation of glycine betaine in the cytoplasm of cells allows growth in hyperosmotic environments of transgenic plants lacking efficient glycine betaine biosynthetic systems (*20*−*26*) and of clinical isolates of a number of human pathogens (*27*−*34*).

Scheme 1

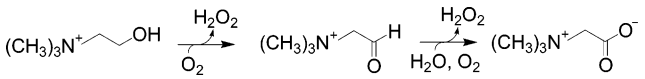

The analyses of the steady-state kinetic mechanism and of the pH and deuterium kinetic isotope effects on the oxidation of choline to betaine aldehyde catalyzed by *Arthrobacter globiformis* choline oxidase were recently reported (*18*, *19*). Briefly, with choline as substrate (lower loop in Scheme 2), after formation of the E-FAD_{ox}-C complex and oxidation of choline to yield betaine aldehyde bound to the reduced enzyme, oxygen reacts with the E-FAD_{red}-BA complex. The catalytically competent E-FAD_{ox}-BA species undergoes a second oxidation reaction in which glycine betaine is formed. Finally, the E-FAD_{red}-GB complex reacts with oxygen before the release of glycine betaine from the oxidized enzyme. With betaine aldehyde

† This work was supported in part by Grant PRF #37351-G4 from the American Chemical Society (GG.) and a Research Initiation Grant and a Quality Improvement Fund from Georgia State University (G.G.).

* Address correspondence to the following author. Phone: (404) 651-4737. Fax: (404) 651-1416. Email: ggadda@gsu.edu.

‡ Department of Chemistry.

§ These authors contributed equally to this study.

|| Department of Biology.

⊥ The Center for Biotechnology and Drug Design.

10.1021/bi035435o CCC: $25.00
Published on Web 12/06/2003

Scheme 2

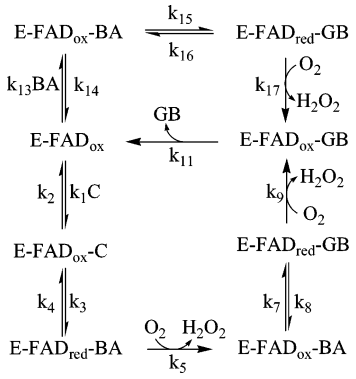

as substrate (upper loop in Scheme 2), after formation of the E-FAD$_{ox}$-BA complex, betaine aldehyde is oxidized to yield glycine betaine bound to the reduced enzyme. Turnover is completed with reaction of the E-FAD$_{red}$-GB complex with molecular oxygen and the final release of the product glycine betaine. A catalytic base with pK_a 7.5 was proposed to participate in catalysis based on pH and substrate kinetic isotope effect studies on the enzyme (*19*).

Our group recently cloned the gene encoding for choline oxidase from genomic DNA of *A. globiformis* strain ATCC 8010 and expressed it to high yields in *Escherichia coli* (*6*). The resulting protein was purified to homogeneity and shown to be a homodimer of 120,000 Da with each subunit containing covalently linked FAD in a mixture of semiquinone and oxidized redox states (*6*). In the present study, we have devised methods to obtain homogeneous preparations of recombinant choline oxidase with the flavin cofactor either in the oxidized or in the semiquinone state and have characterized the biochemical and kinetic properties of the resulting forms of enzyme.

EXPERIMENTAL PROCEDURES

Materials. Choline chloride was from ICN Pharnaceutical, Inc. Betaine aldehyde and glycine betaine were from Sigma-Aldrich. Recombinant choline oxidase from *A. globiformis* strain ATCC 8010 was expressed from plasmid pET/*codA*1 and purified to homogeneity as described in ref *6*. Choline oxidase as purified was stored at −20 °C in 200 mM Tris-Cl, pH 8, and found to be stable for at least six months. All other reagents were of the highest purity commercially available.

Enzyme Assays. The concentration of choline oxidase was determined with the method of Bradford (*35*), by using the Bio-Rad protein assay kit with bovine serum albumin as the standard. Enzyme activity was measured with the method of the initial rates (*36*) in air-saturated 50 mM potassium phosphate at pH 7 by monitoring the rate of oxygen consumption with a computer-interfaced Oxy-32 oxygen-monitoring system (Hansatech Instrument Ltd.) thermostated at 25 °C. The reactions were started by the addition of choline oxidase to a 1 mL reaction mixture, with the final concentration of enzyme in the 0.2−0.6 μM range; the concentration of choline or betaine aldehyde was between 0.02 and 15 mM. When both choline (or betaine aldehyde) and oxygen concentrations were varied, the assay reaction mixture was equilibrated at the concentration of oxygen by bubbling the appropriate O_2/N_2 gas mixture for 10 min before the reaction was started by the addition of the enzyme. When the pH was varied, 50 mM potassium phosphate was used between pH 6 and 8, and 50 mM sodium pyrophosphate was used in the pH ranges 5−6 and 8−10. Product inhibition studies were carried out by varying the concentrations of both glycine betaine and choline (or betaine aldehyde) in air-saturated 50 mM potassium phosphate, pH 6.75. One unit of enzymatic activity corresponds to the consumption of one μmol of oxygen per minute.

UV−vis absorbance spectra were recorded using an Agilent Technologies diode-array spectrophotometer Model HP 8453 equipped with a thermostated water bath. Fluorescence emission spectra were recorded with a Shimadzu Spectrofluorometer Model RF-5301 PC thermostated at 15 °C. Circular dichroism spectra were acquired using a Jasco J-810 spectropolarimeter at 22 °C.

Methods. Oxidized FAD-containing choline oxidase was prepared at 4 °C by dialysis against three 1 L changes of 20 mM potassium phosphate, 20 mM sodium pyrophosphate, pH 6 over 24 h, followed by two 1 L changes of 200 mM Tris-Cl, pH 8 over 5 h. This enzyme could be stored at −20 °C for at least 7 months without losses in enzymatic activity. The oxidized flavin content of choline oxidase as purified was determined from the ΔA_{452} after treatment of the enzyme with 5 mM dithionite in air-saturated 200 mM Tris-Cl, pH 8, using an ϵ_{452} value of 8.4 mM^{-1} cm^{-1}, which corresponds to the difference between the extinction coefficients for the enzyme-bound oxidized flavin (ϵ_{452} = 8.4 mM^{-1} cm^{-1}) and semiquinone flavin (ϵ_{452} = 3 mM^{-1} cm^{-1}). Reduction of choline oxidase with sodium dithionite was conducted aerobically in 200 mM Tris-Cl, pH 8 at 15 °C. Dithionite was either prepared just before use in the same buffer or added to the enzyme solution as a powder. For reactions with sodium sulfite, the reagent was prepared just prior to use as a 1 M stock solution in 100 mM potassium phosphate, pH 7. Different amounts of sodium sulfite ranging from 0.5 to 25 mM were added to the enzyme solution in 100 mM potassium phosphate, pH 7, at 15 °C, and UV−vis absorbance spectra were recorded at different interval periods. Reversibility of the flavin−sulfite complex was determined by following the increase in absorbance at 452 nm following removal of the unbound sulfite by gel filtration using a Sephadex G-25 column (PD-10 column, Amersham-Pharmacia Biotech) equilibrated with 200 mM Tris-Cl, pH 8. For treatment of choline oxidase with an oxidizing agent under nondenaturing conditions, the enzyme was incubated with 10 mM potassium ferricyanide for 30 min on ice in 10% glycerol, 1 mM EDTA, 20 mM Tris-Cl, pH 8 before removing ferricyanide by gel filtration using a Sephadex G-25 column equilibrated with 20 mM Tris-Cl, pH 8.

ESR spectral data were recorded in 3 mm quartz tubes at 141 K using a Bruker ER200D spectrophotometer equipped with an Oxford cryostat. Samples were prepared for ESR analysis by gel filtration through a Sephadex G-25 column equilibrated in 50 mM HEPES, pH 8, followed by freezing in liquid nitrogen. The following conditions and instruments settings were used: microwave power, 2 mW; modulation amplitude, 2 G; and microwave frequency, 9.4 GHz.

Data Analysis. Kinetic data were fit with the KaleidaGraph software (Adalbeck Software, Reading, PA) and the Enzfitter software (Biosoft, Cambridge, UK). Apparent kinetic parameters in atmospheric oxygen were determined by fitting

initial reaction rates at different substrate concentrations to the Michaelis−Menten equation for one substrate. Initial rates determined by varying the concentration of both choline or betaine aldehyde and oxygen were fit to eqs 1 and 2, respectively. Eq 1 describes a sequential steady-state kinetic mechanism, whereas eq 2 describes a sequential mechanism in which $K_a \ll K_{ia}$ (*37*). K_a and K_b are the Michaelis constants for choline (or betaine aldehyde) (A) and oxygen (B), respectively, and k_{cat} is the turnover number of the enzyme (e).

$$\frac{v}{e} = \frac{k_{cat}AB}{K_aB + K_bA + AB + K_{ia}K_b} \quad (1)$$

$$\frac{v}{e} = \frac{k_{cat}AB}{K_bA + AB + K_{ia}K_b} \quad (2)$$

The pH dependences of steady-state kinetic parameters were determined by fitting initial rate data to eq 3, which describes a curve with a slope of +1 and a plateau region at high pH. The pH dependence of inhibition by glycine betaine was determined by fitting the initial rate data to eq 4, which describes a curve with a slope of −1 and a plateau region at low pH. C is the pH-independent value of the kinetic parameter of interest.

$$\log Y = \log\left(\frac{C}{1 + \frac{10^{-pH}}{10^{-pK_a}}}\right) \quad (3)$$

$$\log Y = \log\left(\frac{C}{1 + \frac{10^{-pK_a}}{10^{-pH}}}\right) \quad (4)$$

Product inhibition studies were performed by varying the concentrations of both glycine betaine and choline (or betaine aldehyde) at a fixed concentration of oxygen. The data were fit to eqs 5−7, which describe competitive, uncompetitive, and noncompetitive inhibition patterns of the product and the organic substrate, respectively. P is the concentration of glycine betaine, and K_{is} and K_{ii} are the inhibition constants for the slope and intercept term, respectively.

$$\frac{v}{e} = \frac{k_{cat}A}{K_a\left[1 + \left(\frac{P}{K_{is}}\right)\right] + A} \quad (5)$$

$$\frac{v}{e} = \frac{k_{cat}A}{K_a + A\left[1 + \left(\frac{P}{K_{ii}}\right)\right]} \quad (6)$$

$$\frac{v}{e} = \frac{k_{cat}A}{K_a\left[1 + \left(\frac{P}{K_{is}}\right)\right] + A\left[1 + \left(\frac{P}{K_{ii}}\right)\right]} \quad (7)$$

RESULTS

Choline Oxidase as Purified (E-FAD$_{ox/sq}$). As shown in Figure 1, the UV−vis absorbance spectrum of recombinant choline oxidase as purified at pH 8 suggests that the enzyme-bound FAD is present as a mixture of oxidized and anionic semiquinone states (E-FAD$_{ox/sq}$) (*6*). Upon treatment of the enzyme with 10 mM potassium ferricyanide at pH 8 followed by gel filtration to remove the oxidizing agent, no significant spectral changes in the near-UV and visible regions of the absorbance spectrum were observed (data not shown). These results indicate that the addition of an oxidant under nondenaturing conditions had no effect on the enzyme-bound flavin semiquinone.

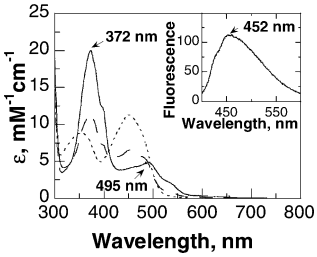

FIGURE 1: Reaction of recombinant choline oxidase with sodium dithionite. Dashed line, the UV−vis absorbance spectrum of choline oxidase as purified was recorded at a concentration of 60 μM in 200 mM Tris-Cl, pH 8; solid line, air-stable flavin semiquinone-containing enzyme prepared by treatment with 5 mM sodium dithionite in aerobiosis and gel filtration onto a Sephadex G-25 column equilibrated with the same buffer; dotted line, after treatment of the flavin semiquinone-containing enzyme with 4 M urea at 40 °C for 40 min. Inset, fluorescence emission spectrum of flavin semiquinone-containing choline oxidase at a concentration of 8 μM in 200 mM Tris-Cl, pH 8 and 15 °C. The excitation wavelength was at 372 nm.

Spectral Properties of Flavin Semiquinone-Containing Choline Oxidase (E-FAD$_{sq}$). When the enzyme was incubated aerobically with 5 mM dithionite, a bleaching of the peak at 454 nm was observed in the visible absorbance spectrum of the enzyme, and a spectrum with maxima at 372 and 495 nm was obtained (data not shown). The ΔA_{452} was used to determine the FAD$_{ox}$ content per enzyme active site by using the ϵ_{452} values determined for the enzyme-bound flavin in the oxidized and semiquinone states (see below). Typically, the enzyme as purified contained variable amounts of flavin in the oxidized state, ranging from 15 to 55% of the total flavin content (data not shown). Removal of excess dithionite by gel filtration yielded a similar absorbance spectrum (Figure 1), indicating that the enzyme is capable of stabilizing the anionic semiquinone species of the flavin (FAD$_{sq}$) in the presence of molecular oxygen. Upon incubation of the FAD$_{sq}$-containing choline oxidase in the presence of 4 M urea, the visible absorbance spectrum of oxidized FAD with the typical peaks centered at 350 and 452 nm was observed (Figure 1), consistent with the FAD$_{sq}$ being stabilized by the protein microenvironment and the cofactor becoming fully oxidized by molecular oxygen upon unfolding the protein. An extinction coefficient of 19.95 mM^{-1} cm^{-1} was calculated at 372 nm for the enzyme-bound semiquinone of choline oxidase based upon the ϵ_{450} value of 11.3 mM^{-1} cm^{-1} for FAD[1] after denaturation of the enzyme by treatment with urea (*38*). At pH 8 and 15 °C, the enzyme-bound anionic semiquinone emitted light at 454 nm upon excitation at 372 nm (Figure 1). As for the case of the visible absorbance spectrum, the typical fluorescence properties of oxidized FAD with maximal emission at 530 nm (with λ_{max} at 450

[1] It is assumed here that the ϵ_{450} for 8α-*N*(1)-histidyl FAD is the same as that for free FAD in solution, with a value of 11.3 mM^{-1} cm^{-1}.

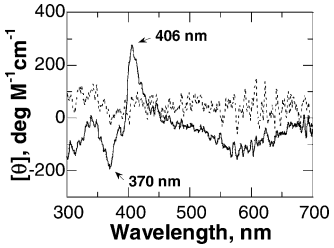

FIGURE 2: Circular dichroism spectrum of flavin semiquinone-containing choline oxidase. Solid line, choline oxidase after treatment with 5 mM sodium dithionite in aerobiosis followed by gel filtration onto a Sephadex G-25 column equilibrated with 200 mM Tris-Cl, pH 8; dotted line, after treatment of the flavin semiquinone-containing enzyme with 4 M urea at 40 °C for 30 min. Spectra were recorded at 22 °C.

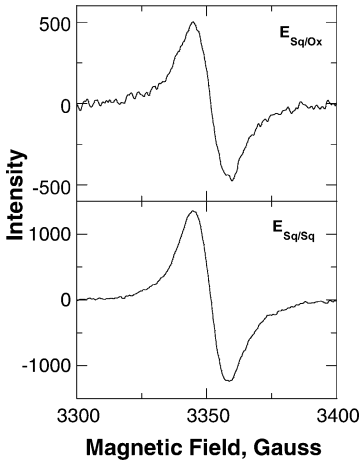

FIGURE 3: Electron spin resonance spectrum of recombinant choline oxidase. Spectra of choline oxidase were acquired at a concentration of 60 μM in 50 mM HEPES, pH 8. The following spectral conditions were used: microwave power, 2 mW; modulation amplitude, 2 G; gain, 6.3×10^5; temperature, 141 K. Panel A, choline oxidase as purified; panel B, flavin semiquinone-containing choline oxidase prepared freshly by the addition of sodium dithionite and gel filtration onto a Sephadex G-25 column.

nm) were observed upon denaturation of the FAD$_{sq}$-containing enzyme by treatment with urea (data not shown). The circular dichroism spectrum of the E-FAD$_{sq}$ form of choline oxidase showed a negative band at 370 nm, a sharp positive band at 406 nm, and a broad negative dichroic signal spanning from 450 to 650 nm (Figure 2). Such a spectrum is in agreement with previously reported circular dichroic spectra of enzyme-bound anionic flavin semiquinones (*39*, *40*).

As an independent approach to characterizing the enzyme-bound semiquinone flavin of choline oxidase, ESR spectra of the enzyme as purified and of the semiquinone-containing enzyme were determined. As shown in Figure 3, E-FAD$_{ox/sq}$ yielded an ESR signal at 2 G with a peak-to-peak line width of 15.4 G, providing further evidence for the presence of an anionic flavin semiquinone in the enzyme (*41*). A similar ESR spectrum with peak line width of 13.9 G was observed when the enzyme was analyzed after treatment with dithionite and gel filtration to remove the excess dithionite, further consistent with the formation of an air-stable anionic semiquinone upon reduction of the enzyme by dithionite.

Spectral Properties of Oxidized FAD-Containing Choline Oxidase (E-FAD$_{ox}$). Treatment of choline oxidase at pH 6 and 15 °C resulted in the slow bleaching of the near-UV band centered at 373 nm and concomitant increase of absorbance at 452 nm (Figure 4). The resulting enzyme species showed absorbance maxima in the near-UV and visible regions centered at 359 and 452 nm, as expected for an enzyme with the bound flavin in the oxidized state (E-FAD$_{ox}$). At 15 °C, a k_{obs} value of $219 \pm 1 \times 10^{-6}$ s^{-1} was determined from the absorbance changes at 452 nm for the complete conversion of E-FAD$_{ox/sq}$ to E-FAD$_{ox}$ (Figure 4, inset). To minimize possible protein losses due to the prolonged incubation of the enzyme at pH 6, E-FAD$_{ox}$ was also prepared by dialysis at 4 °C. When 1300 units of choline oxidase as purified were dialyzed at pH 6 for 24 h, 4100 units of E-FAD$_{ox}$ were recovered, consistent with the formation of E-FAD$_{ox}$ being due to oxidation rather than denaturation of E-FAD$_{sq}$. As shown in Figure 5, an extinction coefficient at 452 nm of 11.4 ± 0.6 mM^{-1} cm^{-1} was calculated for E- FAD$_{ox}$ from six independent experiments after denaturation of the enzyme by treatment with urea. A fluorescence emission spectrum with a maximum at 530 nm (with λ_{ex} at 452 nm) was observed for E-FAD$_{ox}$, providing further evidence for the presence of oxidized FAD. As for the case of the E-FAD$_{ox/sq}$ species, a UV−vis absorbance spectrum identical to that of E-FAD$_{sq}$ was obtained upon aerobic addition of dithionite to E-FAD$_{ox}$ (data not shown).

Formation of a covalent *N*(5)-flavin adduct with sulfite is a feature that distinguishes flavoprotein oxidases from

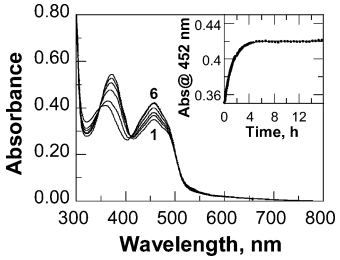

FIGURE 4: Conversion of E-FAD$_{ox/sq}$ to E-FAD$_{ox}$. Choline oxidase as purified at a concentration of 33 μM was incubated in air-saturated buffer at pH 6 and 15 °C. Absorbance spectra were recorded at different times of incubation until no further spectral changes were observed. Only selected spectra are shown: curve 1, absorbance spectrum of choline oxidase recorded 1 min after gel filtration of the enzyme through a Sephadex G-25 column equilibrated with 20 μM potassium phosphate, 20 mM sodium pyrophosphate, pH 6; curve 6, same sample after 15 h of incubation. Inset, time course of absorbance changes at 452 nm. The curve is a fit of the data to $y = 0.420 - 0.071e^{(0.79x)}$ ($R^2 = 0.9997$).

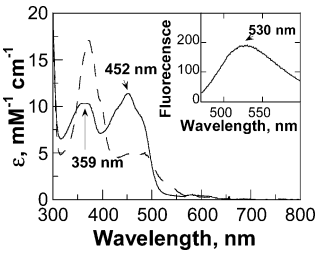

FIGURE 5: Reaction of FAD$_{ox}$-containing choline oxidase with sodium dithionite. Solid line, the UV−vis absorbance spectrum of FAD$_{ox}$-containing choline oxidase was recorded at a concentration of 75 μM in 200 mM Tris-Cl, pH 8; dashed line, air-stable semiquinone-containing enzyme prepared by treatment with 5 mM sodium dithionite in aerobiosis and gel filtration onto a sephadex G-25 column equilibrated with the same buffer. Inset, fluorescence emission spectrum of FAD$_{ox}$-containing choline oxidase at a concentration of 15 μM in 200 mM Tris-Cl, pH 8 and 15 °C. The excitation wavelength was at 453 nm.

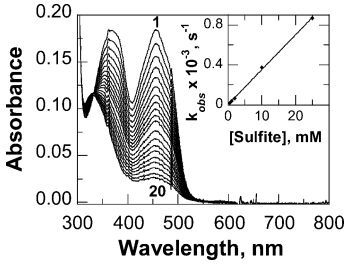

FIGURE 6: Reaction of choline oxidase with sulfite. FAD_{ox}-containing choline oxidase at a concentration of 15 μM was incubated with 25 mM sodium sulfite in air-saturated 100 mM potassium phosphate, pH 7 and 15 °C. Absorbance spectra were recorded at different times of incubation until no further spectral changes were observed. Only selected spectra are shown: curve 1, absorbance spectrum of choline oxidase recorded 10 s after the addition of sulfite; curve 20, same sample after 2 h of incubation. Inset, plot of the observed rate of decrease in absorbance at 452 nm versus the concentration of sulfite. The line is a fit of the data to $y = 0.035x + 0.0000049$ ($R^2 = 0.999$).

dehydrogenases (*42*, *43*). As shown in Figure 6, treatment of FAD_{ox}-containing choline oxidase with sodium sulfite resulted in the bleaching of the peak at 452 nm with the concomitant appearance of a peak centered at 320 nm, consistent with formation of a sulfite *N*(5)-flavin adduct. At pH 7 and 15 °C, complex formation was slow and required several hours for completion at concentrations of sulfite as high as 25 mM. Values for the rate of complex formation (k_{on}) and dissociation (k_{off}) of 0.035 ± 0.001 M^{-1} s^{-1} and 4.9 ± 8.4 × 10^{-6} s^{-1} were calculated from a plot of k_{obs} versus sulfite concentration, respectively (Figure 6, inset). Although a k_{off} value not significantly different from zero was observed, by using the upper limiting k_{off} value of 1.33 × 10^{-5} s^{-1} calculated from the sum of the *y*-intercept value in Figure 5 and the standard deviation associated with the measurement, an upper K_d value of ~40 μM could be estimated from the ratio of the k_{off} to k_{on} values. From a plot of ΔA_{452} versus [sulfite], a K_d value of 51 ± 10 μM was determined from the reaction at various concentrations of sulfite (data not shown), in fairly good agreement with the value determined kinetically. Reversibility of the flavin-sulfite adduct was established by following the increase in absorbance at 452 nm after removing the excess sulfite by gel filtration (data not shown). However, an accurate determination of the k_{off} value could not be carried out due to instability of the enzyme over the prolonged incubation times required for complete sulfite dissociation. Although the slow rates of sulfite complex formation and dissociation observed with choline oxidase are atypical for flavoprotein oxidases, similar results were recently observed for another flavin-linked enzyme, *N*-methyltryptophan oxidase (*44*).

Enzymatic Turnover of E-$FAD_{ox/sq}$, E-FAD_{sq}, and E-FAD_{ox} with Choline. To determine whether the flavin semiquinone of choline oxidase participates in catalysis, choline oxidase containing either $FAD_{ox/sq}$, FAD_{sq}, or FAD_{ox} was incubated with 4 mM choline in air-saturated 200 mM Tris-Cl, at pH 8 and 15 °C. As shown in Figure 7, a UV−vis absorbance spectrum with maxima at 372 and 495 nm was observed with the $FAD_{ox/sq}$-containing enzyme, suggesting that the enzyme-bound oxidized flavin was fully reduced in the presence of the substrate and that the flavin semiquinone did not react with choline or oxygen under enzyme turnover. After removal of the excess choline by gel filtration, a UV−vis absorbance spectrum substantially identical to that of the resting state of E-$FAD_{ox/sq}$ was observed (Figure 7), further consistent with the flavin semiquinone not participating in catalysis. When a freshly prepared sample of the E-FAD_{sq} form of choline oxidase was subjected to the same treatment, no changes were observed in the UV−vis absorbance spectra of both the enzyme under turnover and in the resting state after removal of excess choline by gel filtration (Figure 7), in good agreement with the results observed with the enzyme containing a mixture of oxidized and semiquinone flavins. Finally, a peak centered at 356 nm was observed in the UV−vis absorbance spectrum of the FAD_{ox}-containing enzyme in the presence of choline and oxygen, suggesting that this species of enzyme was fully reduced under these conditions (Figure 7). After removing the excess choline by gel filtration, an absorbance spectrum substantially identical to that of the initial E-FAD_{ox} species in the resting state was observed (Figure 7). Altogether, the results of these experiments are consistent with the flavin semiquinone of choline oxidase being not catalytically competent and with the enzyme-bound flavin cycling between fully oxidized and reduced states during catalytic turnover of the enzyme with the substrates.

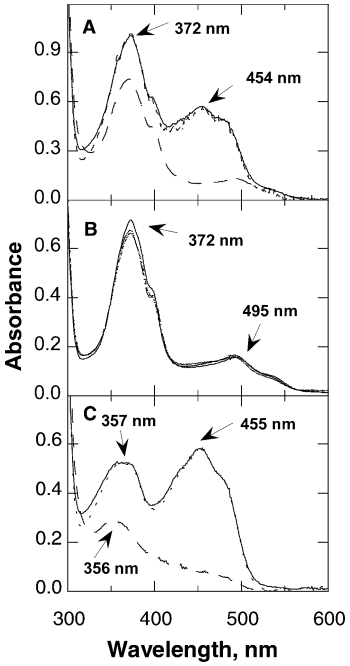

FIGURE 7: UV−vis absorbance spectra of choline oxidase during turnover with choline. Choline oxidase containing different relative amounts of flavin semiquinone and oxidizied flavin was incubated for 30 min with 4 mM choline in air-saturated 100 mM potassium phosphate, pH 7 and 15 °C, before stopping the reaction by gel filtration onto a Sephadex G-25 column equilibrated with the same buffer. UV−vis absorbance spectra were recorded for the enzyme in the resting state before turnover (solid curve), under turnover (dashed curve), and in the resting state after turnover (dotted curve). Panel A, 95 μM choline oxidase containing $FAD_{ox/sq}$; panel B, 50 μM choline oxidase containing FAD_{sq}; and panel C, 79 μM choline oxidase containing FAD_{ox}. Spectra for the resting enzyme after turnover were normalized to those of the resting enzyme before turnover.

Steady-State Kinetics. The steady-state kinetic parameters for recombinant choline oxidase were determined for both the E-FAD_{ox} and the E-$FAD_{ox/sq}$ forms of choline oxidase, by measuring the rate of oxygen consumption at varying

Table 1: Steady-State Kinetic Parameters for Recombinant Choline Oxidase with Choline or Betaine Aldehyde as Substrate at pH 7[a]

substrate	FAD_{ox}/FAD_{total}[b]	k_{cat}, s^{-1} [c]	K_a, mM[d]	k_{cat}/K_a, $M^{-1}\,s^{-1}$ [e]	K_{O2}, μM	k_{cat}/K_{O2}, $M^{-1}\,s^{-1}$	K_{ia}, mM	eq	R^2
choline	1.00	61 ± 6	1.7 ± 0.3	36000 ± 6400	703 ± 102	87100 ± 15300	0.2 ± 0.05	1	0.998
choline	0.37	60 ± 5	2.9 ± 0.3	21000 ± 3000	830 ± 90	72400 ± 9900	0.2 ± 0.03	1	0.999
betaine aldehyde	1.00	69 ± 1			1090 ± 30	64000 ± 2100	2.2 ± 0.09	2	0.998
betaine aldehyde	0.37	67 ± 1			970 ± 1	69000 ± 100	2.3 ± 0.01	2	1.000

[a] Enzyme activity was measured at varying concentrations of both organic substrate and oxygen in 50 mM potassium phosphate, pH 7 and 25 °C. [b] Oxidized flavin content per total enzyme-bound flavin. [c] Rates are expressed per active site oxidized flavin content. [d] K_a is the K_m value for either choline or betaine aldehyde as substrate. [e] k_{cat}/K_a is the k_{cat}/K_m value for either choline or betaine aldehyde as substrate.

Table 2: Product Inhibition Studies of Recombinant Choline Oxidase with Glycine Betaine[a]

substrate	FAD_{ox}/FAD_{total}[b]	type of inhibition[c]	k_{cat}, s^{-1} [d]	K_m, mM	K_{is}, mM	K_{ii}, mM	eq	R^2
choline	1.00	C	10.6 ± 0.2	0.8 ± 0.1	15 ± 1		5	0.999
		UC	11.3 ± 0.2	1.1 ± 0.1		27 ± 1	6	0.929
		NC	9.3 ± 0.4	0.6 ± 0.1	12 ± 2	$10^8 \pm 10^{14}$	7	0.995
	0.37	C	9.7 ± 0.1	0.8 ± 0.1	12 ± 0.3		5	0.993
		UC	9.4 ± 0.1	0.7 ± 0.1		21 ± 0.1	6	0.941
		NC	9.7 ± 0.1	0.8 ± 0.1	12 ± 0.1	$10^8 \pm 10^{11}$	7	0.993
betaine aldehyde	1.00	C	6.1 ± 0.1	2.0 ± 0.1	56 ± 2		5	0.991
		UC	10.0 ± 0.1	5.0 ± 0.1		41 ± 2	6	0.971
		NC	7.6 ± 0.7	2.8 ± 0.7	51 ± 26	$10^3 \pm 10^4$	7	0.960
	0.37	C	5.9 ± 0.1	2.6 ± 0.1	48 ± 4		5	0.996
		UC	7.8 ± 0.1	4.0 ± 0.1		29 ± 1	6	0.982
		NC	7.2 ± 0.3	3.3 ± 0.4	49 ± 11	755 ± 926	7	0.993

[a] Enzyme activity was measured at varying concentrations of organic substrate and glycine betaine in air-saturated 50 mM potassium phosphate, pH 6.75 and 25 °C. [b] Oxidized flavin content per total enzyme-bound flavin. [c] C, competitive; UC, uncompetitive, and NC, noncompetitive. [d] Rates are expressed per active site oxidized flavin content.

concentrations of both organic substrate and oxygen at pH 7 and 25 °C. As expected based on previous studies on *A. globiformis* choline oxidase (*18*), the kinetic data with choline and betaine aldehyde were fit best by eqs 1 and 2, which describe sequential kinetic mechanisms with finite and negligible K_a values, respectively (*37*). As shown in Table 1, when the kinetic parameters were expressed per active site of oxidized flavin content, no significant differences were observed in the k_{cat} and k_{cat}/K_m values when enzyme forms with different FAD_{ox}/FAD_{total} ratios were compared, providing independent evidence that the flavin semiquinone of choline oxidase does not participate in catalysis.[2]

Product Inhibition Studies. As an independent approach to examining the steady-state kinetic mechanism of recombinant choline oxidase, the inhibition patterns of the product glycine betaine with respect to either choline or betaine aldehyde were determined in air-saturated buffer at pH 6.75. As shown in Table 2, the results were best fit by eq 5, consistent with glycine betaine being competitive versus either choline or betaine aldehyde. Moreover, similar kinetic parameters were obtained irrespective of the use of $E\text{-}FAD_{ox/sq}$ or $E\text{-}FAD_{ox}$ when the initial rates were expressed per active site of oxidized flavin (Table 2).

pH Dependence of the k_{cat} and k_{cat}/K_m Values. The pH dependence of the kinetic parameters with choline as substrate was determined at varying concentrations of both choline and oxygen in the pH range 6−10. As shown in Figure 8, both the k_{cat}/K_m and the k_{cat} values for choline increased with increasing pH, reaching limiting values above pH 8. Apparent pK_a values of 7.6 ± 0.2 and 7.1 ± 0.2 were determined for a group that must be unprotonated for catalysis from the k_{cat}/K_m and k_{cat} pH profiles, respectively. In contrast, the k_{cat}/K_m values for oxygen were independent of pH, with values in the 10^4 $M^{-1}\,s^{-1}$ range (Figure 9).

To establish whether a measurable K_m value could be determined with betaine aldehyde as substrate for the enzyme, initial rates of reaction were measured at pH 6.5 and 10 by varying the concentrations of both betaine aldehyde and oxygen. At both pH values, the data were fit best to eq 2 (data not shown), consistent with k_{cat} being independent of the concentration of betaine aldehyde (*37*). The k_{cat} values with betaine aldehyde were 42 ± 2 s^{-1} at pH 6.5 and 70 ± 1 s^{-1} at pH 10. As for the case of choline, the k_{cat}/K_m values for oxygen determined with betaine aldehyde as the organic substrate were independent of the pH (Figure 9).

As an approach to establishing whether some changes in the kinetic properties of the enzyme take place in the conversion of $E\text{-}FAD_{ox/sq}$ to $E\text{-}FAD_{ox}$, the pH dependences of the kinetic parameters with choline as substrate for both enzyme species were determined in air-saturated buffer in the pH range from 5 to 10. As shown in Figure 10, both the k_{cat}/K_m and the k_{cat} values yielded similar pH profiles irrespective of whether the $E\text{-}FAD_{ox}$ or $E\text{-}FAD_{ox/sq}$ species

[2] If the flavin semiquinone were as catalytically competent as the oxidized flavin in the reaction catalyzed by choline oxidase, similar k_{cat} and k_{cat}/K_m values should have been obtained by expressing the enzymatic activity per active site total flavin content. Alternatively, if the flavin semiquinone were either less or more catalytically competent than the oxidized flavin, due to the kinetic complexity of the reaction catalyzed by choline oxidase, significantly different k_{cat}, K_m, K_{ia}, and k_{cat}/K_m values should have been observed irrespective of whether the enzymatic activity is expressed per active site oxidized flavin content or total flavin content. Within experimental error, the kinetic results observed with enzyme forms containing different relative amounts of flavin semiquinone and oxidized flavin are therefore consistent with the conclusion that the oxidized flavin is solely responsible for catalytic activity.

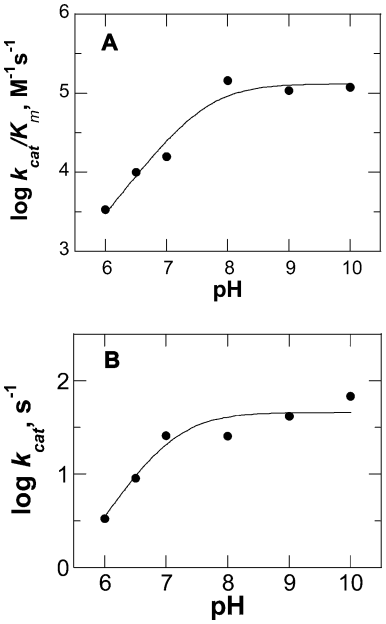

FIGURE 8: pH dependence of the k_{cat}/K_m and k_{cat} values for choline as substrate for recombinant choline oxidase. Choline oxidase activity was measured at varying concentration of both choline and oxygen at 25 °C as described in the Experimental Procedures. The lines are fits of the data to eq 3. Panel A, pH dependence of the k_{cat}/K_m values; panel B, pH dependence of the k_{cat} values.

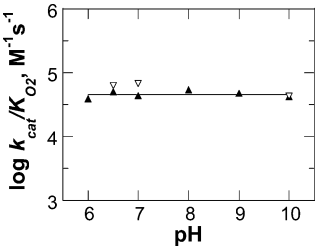

FIGURE 9: pH dependence of the k_{cat}/K_m values for oxygen with choline or betaine aldehyde as substrate for recombinant choline oxidase. Choline oxidase activity was measured at varying concentrations of both choline (or betaine aldehyde) and oxygen at 25 °C as described in the Experimental Procedures. (▼) Values determined with choline; (△) values determined with betaine aldehyde. The line represents the average pH-independent k_{cat}/K_m value with choline as substrate.

was used, indicating that no changes other than the oxidation of E-FAD_{sq} occur in the preparation of E-FAD_{ox} by treatment at pH 6. The pK_a values were 7.4 ± 0.1 and 7.3 ± 0.1 in the k_{cat}/K_m pH profiles and 6.4 ± 0.1 and 6.6 ± 0.1 in the k_{cat} pH profiles with E-FAD_{ox} and E-$FAD_{ox/sq}$, respectively, in agreement with the values of 7.2 ± 0.2 and 6.4 ± 0.1 recently determined for choline oxidase from *A. globiformis* (*19*).

pH Dependence of Inhibition by Glycine Betaine. The pH dependence of the inhibition by glycine betaine was determined in atmospheric oxygen using choline as substrate for E-FAD_{ox}. As shown in Figure 11, the data were fit best by eq 4, consistent with a single ionizable group with a pK_a value of 7.5 ± 0.1 that must be protonated for inhibition.

DISCUSSION

Recombinant choline oxidase expressed in *E. coli* cells contains between 35 and 85% of bound flavin in an anionic semiquinone form that requires the protein microenvironment to be stabilized. At pH 8, this enzyme-bound flavosemi-

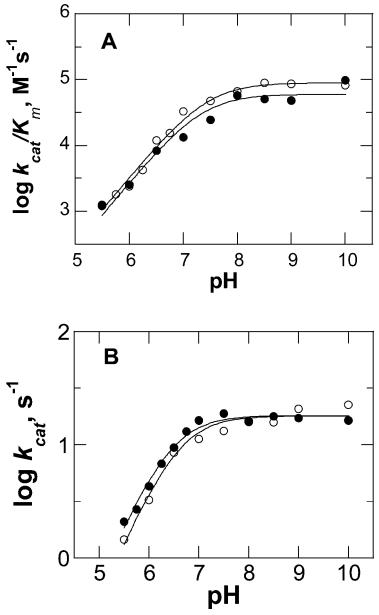

FIGURE 10: pH dependence of the apparent kinetic parameters of E-$FAD_{ox/sq}$ and E-FAD_{ox} with choline as substrate. Choline oxidase activity was measured in air-saturated buffer at 25 °C. (●) Values determined with E-FAD_{ox}; (○) values determined with E-$FAD_{ox/sq}$. The lines are fits of the data to eq 3. Panel A, pH dependence of the k_{cat}/K_m values; panel B, pH dependence of the k_{cat} values.

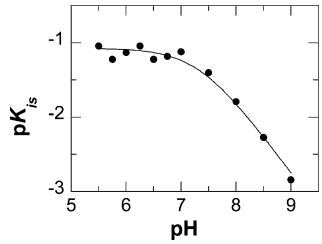

FIGURE 11: pH dependence of inhibition by glycine betaine. At each pH value, choline oxidase activity was measured at varying concentrations of both choline and glycine betaine in air-saturated buffer at 25 °C. The K_{is} values for glycine betaine were determined by fitting the initial rate data to eq 5. The line is a fit of the data to eq 4.

quinone is unusually insensitive to both molecular oxygen[3] and oxidizing agent ferricyanide, suggesting that the unpaired electron is localized in a region of the flavin that is not accessible for reaction. Earlier studies on native choline oxidase from *Alcaligenes* sp. showed that an anionic semiquinone that was poorly reactive toward oxygen is stabilized by the enzyme (*45*), suggesting that this property does not arise from the expression of the recombinant enzyme in the heterologous system used in our study. A rationale for the unusual air stability of the flavin semiquinone can be proposed based on recent ab initio theoretical calculations, showing that most of the spin density in anionic flavin semiquinones is distributed on either the benzene ring or the *N*(5) position of the flavin (*46*, *47*). The flavin *N*(5) locus is expected to be freely accessible to oxygen because of the role it plays in catalysis by accepting the hydride equivalent generated in the oxidation of the substrate. In contrast, the

[3] The rate of reaction with oxygen of anionic flavin semiquinones in solution is almost diffusion-controlled, with second-order rate constant values of 10^8 M^{-1} s^{-1} (*70*, *71*). That for enzyme-bound anionic semiquinones has been reported for glucose oxidase to be in the 10^4 M^{-1} s^{-1} range (*50*).

benzene ring of FAD is involved in a 8α-*N*(1)-histidyl linkage with the protein (*4*) and is likely to be hindered by the protein moiety. Stabilization of the spin density on the benzene ring of the anionic semiquinone might further be contributed by the inductive effect of the flavin 8α-*N*(1)-histidyl linkage with the protein moiety.

The choline oxidase-bound semiquinone undergoes a slow conversion to the fully oxidized state at pH 6, indicating that a 100-fold increase in proton concentration significantly destabilizes the flavin radical. Although not investigated further in this study, a possible rationale for the oxidation of the flavin semiquinone in choline oxidase is that at low pH a limited fraction of the enzyme-bound semiquinone becomes protonated to yield the neutral species of the semiquinone, which would be readily oxidized by molecular oxygen because of localization of the unpaired electron on the highly oxygen-reactive *C*(4a) locus of the flavin (*43*). pH-dependent stabilization of both anionic and neutral flavin semiquinones by the same enzyme was previously shown in another member of the GMC oxidoreductase superfamily, glucose oxidase (*48*, *49*), for which it was shown that the neutral semiquinone reacts with oxygen with a second-order rate constant of 1.4×10^4 M^{-1} s^{-1} at 25 °C (*50*). Unusual stabilization of neutral semiquinones by flavoprotein oxidases was also reported for nitroalkane oxidase (*51*) and D-amino acid oxidase in the presence of benzoic acid (*52*).

The spectral studies of the enzyme under turnover establish that the flavin semiquinone of choline oxidase is not catalytically relevant and that the enzyme under turnover cycles between its fully oxidized and fully reduced states. This conclusion is further supported by kinetic data, showing a good correlation between the turnover numbers of the enzyme with choline and betaine aldehyde as substrate and the content of oxidized flavin per active site. Consistent with the lack of catalytic role for the flavin semiquinone, variable FAD_{ox}/FAD_{sq} ratios for the enzyme-bound flavin are observed among different preparations of enzyme (*6*). Thus, choline oxidase appears to be similar to methanol oxidase, which was shown in earlier studies to contain a mixture of oxidized FAD and an air-stable anionic semiquinone that is not required for catalysis (*53*). In contrast, air-stable flavin semiquinones for which a catalytic role of the flavin radical was proposed (*54*, *55*) were reported in the resting state of monoamine oxidase B (*56*−*58*) and *E. coli* DNA photolyase (*59*, *60*).

A weak positive charge is located in the active site of choline oxidase in proximity of the N(1)−C(2)═O locus of FAD, as suggested by both the stabilization of the anionic semiquinone and the high affinity of the enzyme for sulfite (*43*). By analogy with other members of the GMC oxidoreductase superfamily whose three-dimensional structure is available, such as glucose oxidase (*61*, *62*), cholesterol oxidase (*63*, *64*), and cellobiose dehydrogenase (*65*), it is likely that the positive charge in choline oxidase is provided by the dipole of an α-helix.

A steady-state kinetic analysis of choline oxidase from *A. globiformis* was recently reported at pH 7 (*18*). The results of the kinetic studies reported here indicate that recombinant and native choline oxidase share identical steady-state sequential mechanisms in which the products are released from the oxidized enzyme (Scheme 2), and most importantly, that the order of the kinetic steps involving substrate binding and product release is not affected by pH. Independent evidence for product release occurring after reaction of the reduced enzyme with oxygen is provided by the competitive inhibition patterns observed with glycine betaine versus both choline and betaine aldehyde. The product inhibition patterns observed in this study also rule out possible kinetically relevant conformational changes occurring after release of the product from the enzyme active site, such as those observed with nitroalkane oxidase (*66*).

His-466 with a pK_a value of 7.5 was recently proposed to participate in catalysis by accepting the hydroxyl proton of choline, based on pH dependence studies in atmospheric oxygen with choline oxidase from *A. globiformis* and sequence alignment comparison with other members of the GMC enzyme superfamily (*19*). Consistent with those results, an amino acid residue with a pK_a value of 7.6 is seen in the k_{cat}/K_m pH profile of recombinant choline oxidase determined at varying concentrations of choline and oxygen. In the kinetic mechanism of Scheme 2, the k_{cat}/K_m value for choline is a combination of rate constants reflecting substrate binding, k_1 and k_2, the catalytic step in which choline is oxidized to betaine aldehyde, k_3 and k_4, and the kinetic step in which the reduced enzyme−product complex is oxidized by oxygen, k_5, as illustrated by eq 8. This raises the possibility that the catalytic base may be involved in oxygen reduction rather than in substrate oxidation. However, the observation that the k_{cat}/K_m values for oxygen are independent of pH unequivocally establishes the involvement of the catalytic base in the oxidation of choline to betaine aldehyde.

$$\frac{k_{cat}}{K_m} = \frac{k_1 k_3 k_5 [O_2]}{k_2 k_4 + k_2 k_5 [O_2] + k_3 k_5 [O_2]} \qquad (8)$$

The pK_a value of 7.5 seen in the pH profile of glycine betaine inhibition is due to an amino acid residue that must be protonated for product binding, as expected if this residue is involved in binding the caboxylate moiety of glycine betaine. This amino acid group is likely to be the same histidine residue that must be unprotonated for catalysis and is responsible for the pK_a value of 7.6 observed in the k_{cat}/K_m pH profile. Since pK_a values determined with competitive inhibitors are expected to reflect true equilibrium dissociation constants, these results establish choline as a slow substrate with little if any external forward commitment to catalysis (*67*). This conclusion does not agree with that recently

[4] In the kinetic mechanism of Scheme 2, the observed isotope effect on the k_{cat}/K_m value is given by

$$\frac{^{D}k_{cat}}{K_m} = \frac{^{D}k_3 + \frac{k_3}{k_2} + 1.24\frac{k_4}{k_5[O_2]}}{1 + \frac{k_3}{k_2} + \frac{k_4}{k_5[O_2]}}$$

(*67*), where 1.24 is the value for the equilibrium kinetic isotope effect for the conversion of an alcohol to an aldehyde (*72*). If the forward commitment to catalysis k_3/k_2 is negligible, any decrease in the observed kinetic isotope effect must be due to the reverse commitment to catalysis $k_4/k_5[O_2]$, which depends on the concentration of oxygen. Since choline oxidase from *A. globiformis* has a K_m value for oxygen of 0.6 mM at pH 7 and 19 °C (*18*), and the concentration of oxygen in air-saturated buffers at 19 °C is ∼0.3 mM, it follows that under these conditions, the rate of oxidation of the enzyme-bound reduced flavin becomes significantly slow. Consequently, a significant increase in the reverse commitment to catalysis is expected at concentrations of oxygen well below saturation in the enzyme-catalyzed oxidation of choline.

reported for choline oxidase from *A. globiformis* based on pH and kinetic isotope effects studies using [1,2-$^2H_4$]-choline in atmospheric oxygen, showing a decrease in the $^Dk_{cat}/K_m$ values with increasing pH (*19*). A reasonable explanation that accounts for all the available data is that the decrease in the apparent $^Dk_{cat}/K_m$ values with increasing pH when the concentration of oxygen is well below saturation is not due to choline being a fast substrate for the enzyme as originally proposed (*19*) but to the reverse catalytic step (k_4 in Scheme 2) becoming significantly fast as compared to the kinetic step in which the enzyme-bound reduced flavin is oxidized (k_5 in Scheme 2).[4]

No ionizable groups with a pK_a value in the pH range from 6 to 10 are required for oxygen reduction in the betaine aldehyde- or glycine betaine-choline oxidase complexes, as suggested by the pH independence of the k_{cat}/K_m values for oxygen with either choline or betaine aldehyde as substrate. These data are consistent with a hydrophobic environment being required for flavin activation in the reduced enzyme−product complexes. In this respect, a hydrophobic channel that may serve as an entrance for oxygen to the active site was recently proposed for another member of the GMC oxidoreductase superfamily, cholesterol oxidase (*68*). Oxygen reactivity in choline oxidase therefore appears to be different from that of glucose oxidase, for which protonation of the active site His-516 residue was recently shown to increase the reactivity of the reduced enzyme toward oxygen by about 4 orders of magnitude (*69*).

In summary, the results of the studies on choline oxidase presented herein have established that the enzyme is a typical flavoprotein oxidase, showing formation of an anionic flavin semiquinone and reactivity with sulfite. However, stabilization of the flavin semiquinone by the enzyme is unusual in that it occurs in the presence of molecular oxygen. Such a lack of reactivity toward oxygen has allowed a spectroscopic characterization of the enzyme-bound anionic flavin semiquinone and to establish that the flavin semiquinone does not participate in catalysis. From a mechanistic standpoint, the kinetic data presented here have indicated that the recently proposed catalytic base of choline oxidase, His-466, participates in the oxidation of the organic substrate but not in the reduction of molecular oxygen.

ACKNOWLEDGMENT

The authors thank Dr. Dale E. Edmondson and Ms. Manuela Trani at the Department of Biochemistry of Emory University, Atlanta, for the electron spin resonance spectral analyses; Dr. Yiming Ye for his assistance in the circular dichroism spectral analyses; and the reviewers for their insightful suggestions.

REFERENCES

1. Ikuta, S., Imamura, S., Misaki, H., and Horiuti, Y. (1977) *J. Biochem. (Tokyo) 82*, 1741−9.
2. Ohishi, N., and Yagi, K. (1979) *Biochem. Biophys. Res. Commun. 86*, 1084−8.
3. Ohta-Fukuyama, M., Miyake, Y., Emi, S., and Yamano, T. (1980) *J. Biochem. (Tokyo) 88*, 197−203.
4. Rand, T., Halkier, T., and Hansen, O. C. (2003) *Biochemistry 42*, 7188−94.
5. Cavener, D. R. (1992) *J. Mol. Biol. 223*, 811−4.
6. Fan, F., Ghanem, M., and Gadda, G. (2003) *Arch. Biochem. Biophys.*, in press.
7. Eccleston, E. D., Thayer, M. L., and Kirkwood, S. (1979) *J. Biol. Chem. 254*, 11399−404.
8. Görisch, H. (1979) *Biochem. J. 181*, 153−7.
9. Burger, E., and Görisch, H. (1981) *Eur. J. Biochem. 118*, 125−30.
10. Burger, E., and Görisch, H. (1981) *Eur. J. Biochem. 116*, 137−42.
11. Grubmeyer, C. T., Chu, K. W., and Insinga, S. (1987) *Biochemistry 26*, 3369−73.
12. Grubmeyer, C. (1991) *Adv. Exp. Med. Biol. 284*, 105−12.
13. Kheirolomoom, A., Mano, J., Nagai, A., Ogawa, A., Iwasaki, G., and Ohta, D. (1994) *Arch. Biochem. Biophys. 312*, 493−500.
14. Nagai, A., and Ohta, D. (1994) *J. Biochem. (Tokyo) 115*, 22−5.
15. Grubmeyer, C., and Teng, H. (1999) *Biochemistry 38*, 7355−62.
16. Teng, H., and Grubmeyer, C. (1999) *Biochemistry 38*, 7363−71.
17. Barbosa, J. A., Sivaraman, J., Li, Y., Larocque, R., Matte, A., Schrag, J. D., and Cygler, M. (2002) *Proc. Natl. Acad. Sci. U.S.A. 99*, 1859−64.
18. Gadda, G. (2003) *Biochim. Biophys. Acta 1646*, 112−8.
19. Gadda, G. (2003) *Biochim. Biophys. Acta 1650*, 4−9.
20. Sakamoto, A., Alia, Murata, N., and Murata, A. (1998) *Plant Mol. Biol. 38*, 1011−9.
21. Sakamoto, A., Valverde, R., Alia, Chen, T. H., and Murata, N. (2000) *Plant J. 22*, 449−53.
22. Alia, Kondo, Y., Sakamoto, A., Nonaka, H., Hayashi, H., Saradhi, P. P., Chen, T. H., and Murata, N. (1999) *Plant Mol. Biol. 40*, 279−88.
23. Hölmstrom, K. O., Somersalo, S., Mandal, A., Palva, T. E., and Welin, B. (2000) *J. Exp Bot. 51*, 177−85.
24. Alia, Hayashi, H., Sakamoto, A., and Murata, N. (1998) *Plant J. 16*, 155−61.
25. Deshnium, P., Gombos, Z., Nishiyama, Y., and Murata, N. (1997) *J. Bacteriol. 179*, 339−44.
26. Deshnium, P., Los, D. A., Hayashi, H., Mustardy, L., and Murata, N. (1995) *Plant Mol. Biol. 29*, 897−907.
27. Bae, J. H., Anderson, S. H., and Miller, K. J. (1993) *Appl. Environ. Microbiol. 59*, 2734−6.
28. Culham, D. E., Emmerson, K. S., Lasby, B., Mamelak, D., Steer, B. A., Gyles, C. L., Villarejo, M., and Wood, J. M. (1994) *Can. J. Microbiol. 40*, 397−402.
29. Graham, J. E., and Wilkinson, B. J. (1992) *J. Bacteriol. 174*, 2711−6.
30. Kaenjak, A., Graham, J. E., and Wilkinson, B. J. (1993) *J. Bacteriol. 175*, 2400−6.
31. Le Rudulier, D., and Bouillard, L. (1983) *Appl. Environ. Microbiol. 46*, 152−9.
32. Le Rudulier, D., Bernard, T., Goas, G., and Hamelin, J. (1984) *Can. J. Microbiol. 30*, 299−305.
33. Pichereau, V., Bourot, S., Flahaut, S., Blanco, C., Auffray, Y., and Bernard, T. (1999) *Microbiology 145*, 427−35.
34. Peddie, B. A., Wong-She, J., Randall, K., Lever, M., and Chambers, S. T. (1998) *FEMS Microbiol. Lett. 160*, 25−30.
35. Bradford, M. M. (1976) *Anal. Biochem. 72*, 248−54.
36. Allison, D. R., and Purich, D. L. (1979) in *Methods in Enzymology* (Purich, D. L., Ed.) pp 3−19, Academic Press, New York.
37. Segel, I. H. (1975) *Enzyme Kinetics*, John Wiley & Sons, Inc., New York.
38. Whitby, L. G. (1953) *Biochem. J. 54*, 437−42.
39. Edmondson, D. E., and Tollin, G. (1971) *Biochemistry 10*, 113−24.
40. Ohta-Fukuyama, M., Miyake, Y., Shiga, K., Nishina, Y., Watari, H., and Yamano, T. (1980) *J. Biochem. (Tokyo) 88*, 205−9.
41. Edmondson, D. E., Ackrell, B. A., and Kearney, E. B. (1981) *Arch. Biochem. Biophys. 208*, 69−74.
42. Massey, V., Muller, F., Feldberg, R., Schuman, M., Sullivan, P. A., Howell, L. G., Mayhew, S. G., Matthews, R. G., and Foust, G. P. (1969) *J. Biol. Chem. 244*, 3999−4006.
43. Massey, V., and Hemmerich, P. (1980) *Biochem. Soc. Trans. 8*, 246−57.
44. Khanna, P., and Schuman Jorns, M. (2001) *Biochemistry 40*, 1451−9.
45. Ohta, M., Miura, R., Yamano, T., and Miyake, Y. (1983) *J. Biochem. (Tokyo) 94*, 879−92.
46. Garcia, J. I., Medina, M., Sancho, J., Alonso, P. J., Gomez-Moreno, C., Mayoral, J. A., and Martinez, J. I. (2002) *J. Phys. Chem. 106*, 4729−35.
47. Zheng, Y. J., and Ornstein, R. L. (1996) *J. Am. Chem. Soc. 118*, 9402−8.
48. Massey, V., and Palmer, G. (1966) *Biochemistry 5*, 3181−9.

49. Massey, V., Brumby, P. E., Komai, H., and Palmer, G. (1969) *J. Biol. Chem. 244*, 1682−91.
50. Stankovich, M. T., Schopfer, L. M., and Massey, V. (1978) *J. Biol. Chem. 253*, 4971−4979.
51. Gadda, G., and Fitzpatrick, P. F. (1998) *Biochemistry 37*, 6154−64.
52. Yagi, K., Takai, A., and Oishi, N. (1972) *Biochim. Biophys. Acta 289*, 37−43.
53. Mincey, T., Tayrien, G., Mildvan, A. S., and Abeles, R. H. (1980) *Proc. Natl. Acad. Sci. U.S.A. 77*, 7099−101.
54. Silverman, R. B. (1995) *Acc. Chem. Res. 28*, 335−42.
55. Jorns, M. S., Wang, B., and Jordan, S. P. (1987) *Biochemistry 26*, 6810−6.
56. Yue, K. T., Bhattacharyya, A. K., Zhelyaskov, V. R., and Edmondson, D. E. (1993) *Arch. Biochem. Biophys. 300*, 178−85.
57. Woo, J. C., and Silverman, R. B. (1994) *Biochem. Biophys. Res. Commun. 202*, 1574−8.
58. DeRose, V. J., Woo, J. C., Hawe, W. P., Hoffman, B. M., Silverman, R. B., and Yelekci, K. (1996) *Biochemistry 35*, 11085−91.
59. Kay, C. W., Feicht, R., Schulz, K., Sadewater, P., Sancar, A., Bacher, A., Mobius, K., Richter, G., and Weber, S. (1999) *Biochemistry 38*, 16740−8.
60. Payne, G., Heelis, P. F., Rohrs, B. R., and Sancar, A. (1987) *Biochemistry 26*, 7121−7.
61. Hecht, H. J., Kalisz, H. M., Hendle, J., Schmid, R. D., and Schomburg, D. (1993) *J. Mol. Biol. 229*, 153−72.
62. Wohlfahrt, G., Witt, S., Hendle, J., Schomburg, D., Kalisz, H. M., and Hecht, H. J. (1999) *Acta Crystallogr., Sect. D. 55*, 969−77.
63. Vrielink, A., Lloyd, L. F., and Blow, D. M. (1991) *J. Mol. Biol. 219*, 533−54.
64. Li, J., Vrielink, A., Brick, P., and Blow, D. M. (1993) *Biochemistry 32*, 11507−15.
65. Hallberg, B. M., Henriksson, G., Pettersson, G., and Divne, C. (2002) *J. Mol. Biol. 315*, 421−34.
66. Gadda, G., and Fitzpatrick, P. F. (2000) *Biochemistry 39*, 1400−5.
67. Cook, P. F., and Cleland, W. W. (1981) *Biochemistry 20*, 1797−805.
68. Coulombe, R., Yue, K. Q., Ghisla, S., and Vrielink, A. (2001) *J. Biol. Chem. 276*, 30435−41.
69. Roth, J. P., and Klinman, J. P. (2003) *Proc. Natl. Acad. Sci. U.S.A. 100*, 62−7.
70. Vaish, S. P., and Tollin, G. (1971) *Bioenergetics 2*, 61−72.
71. Faraggi, M., Hemmerich, P., and Pecht, I. (1975) *FEBS Lett.* 51, 47−51.
72. Cleland, W. W. (1980) in *Methods in Enzymology* (Purich, D. L., Ed.) Vol. 64, pp 104−125, Academic Press, San Diego.

BI035435O